

Missing Value Imputation on Multidimensional Time Series

Parikshit Bansal
IIT Bombay
parikshitb52@gmail.com

Prathamesh Deshpande
IIT Bombay
pratham@cse.iitb.ac.in

Sunita Sarawagi
IIT Bombay
sunita@iitb.ac.in

ABSTRACT

We present DeepMVI, a deep learning method for missing value imputation in multidimensional time-series datasets. Missing values are commonplace in decision support platforms that aggregate data over long time stretches from disparate sources, and reliable data analytics calls for careful handling of missing data. One strategy is imputing the missing values, and a wide variety of algorithms exist spanning simple interpolation, matrix factorization methods like SVD, statistical models like Kalman filters, and recent deep learning methods. We show that often these provide worse results on aggregate analytics compared to just excluding the missing data.

DeepMVI uses a neural network to combine fine-grained and coarse-grained patterns along a time series, and trends from related series across categorical dimensions. After failing with off-the-shelf neural architectures, we design our own network that includes a temporal transformer with a novel convolutional window feature, and kernel regression with learned embeddings. The parameters and their training are designed carefully to generalize across different placements of missing blocks and data characteristics.

Experiments across nine real datasets, four different missing scenarios, comparing seven existing methods show that DeepMVI is significantly more accurate, reducing error by more than 50% in more than half the cases, compared to the best existing method. Although slower than simpler matrix factorization methods, we justify the increased time overheads by showing that DeepMVI is the only option that provided overall more accurate analytics than dropping missing values.

PVLDB Reference Format:

Parikshit Bansal, Prathamesh Deshpande, and Sunita Sarawagi. Missing Value Imputation on Multidimensional Time Series. PVLDB, 14(1): XXX-XXX, 2020.
doi:XX.XX/XXX.XX

PVLDB Availability Tag:

The source code of this research paper has been made publicly available at http://vldb.org/pvldb/format_vol14.html.

1 INTRODUCTION

In this paper we present a system for imputing missing values across multiple time series occurring in multidimensional databases. Examples of such data include sensor recordings along time of different types of IoT devices at different locations, daily traffic logs of web pages from various device types and regions, and demand

along time for products at different stores. Missing values are commonplace in analytical systems that integrate data from multiple sources over long periods of time. Data may be missing because of errors or breakdowns at various stages of the data collection pipeline ranging from faulty recording devices to deliberate obfuscation. Analysis on such incomplete data may yield biased results misinforming data interpretation and downstream decision making. Therefore, missing value imputation is an essential tool in any analytical systems [2, 9, 17, 20].

Many techniques exist for imputing missing values in time-series datasets including several matrix factorization techniques [1, 10, 18, 19, 23, 27], statistical temporal models [13], and recent deep learning methods [3, 7]. Unfortunately, even the best of existing techniques still incur high imputation errors. We show that top-level aggregates used in analytics could get worse after imputation with existing methods, compared to discarding missing data parts before aggregation. Inspired by the recent success of deep learning in other data analytical tasks like entity matching, entity extraction, and time series forecasting, we investigate if better deep learning architectures can reduce this gap for the missing value imputation task.

The pattern of missing blocks in a time series dataset can be quite arbitrary and varied. Also, datasets could exhibit very different characteristics in terms of the length and number of series, amount of repetitions (seasonality) in a series, and correlations across series. An entire contiguous block of entries might be missing within a time series, and/or across multiple time-series. The signals from the rest of the dataset that are most useful for imputing a missing block would depend on the size of the block, its position relative to other missing blocks, patterns within a series, and correlation (if any) with other series in the dataset. If a single entry is missing, interpolation with immediate neighbors might be useful. If a range of values within a single time series is missing, repeated patterns within the series and trends from correlated series might be useful. If the same time range across several series is missing, only patterns within a series will be useful.

Existing methods based on matrix factorization can exploit across series correlations but are not as effective in combining both within series and across series patterns. Modern deep learning methods because of their higher capacity and flexibility can in principle combine diverse signals, particularly when trained end to end with an objective of minimizing imputation errors on set-aside fraction of the known values. However, designing a neural architecture whose parameters can be trained accurately and scalably across diverse datasets and missing patterns proved to be non-trivial. Existing solutions based on popular architectures for sequence data, such as recurrent neural networks (RNNs) have been shown to be worse both in terms of accuracy and running time. We explored a number of alternative architectures spanning Transformers, CNNs, and Kernel methods. A challenge we faced when training a network

This work is licensed under the Creative Commons BY-NC-ND 4.0 International License. Visit <https://creativecommons.org/licenses/by-nc-nd/4.0/> to view a copy of this license. For any use beyond those covered by this license, obtain permission by emailing info@vldb.org. Copyright is held by the owner/author(s). Publication rights licensed to the VLDB Endowment.

Proceedings of the VLDB Endowment, Vol. 14, No. 1 ISSN 2150-8097.
doi:XX.XX/XXX.XX

to combine a disparate set of potentially useful signals was that, the network was quick to overfit on easy signals. Whereas robust imputation requires that the network harness all available signals. After several iterations, we converged on a network design, that we call DeepMVI that is particularly suited to the missing value imputation task.

DeepMVI provides a unified model to incorporate both patterns along time and related time-series along each categorical dimension. The distinctive features of DeepMVI design are:

- (1) A Temporal Transformer model to capture within-series signal via self-attentions as against RNN states.
- (2) A new method of creating Query, Key values for self-attention using convolutional features of left and right window.
- (3) Simultaneous prediction for all positions of a time-series — multiple loss terms per series provides more efficient training than masking based designs used in transformers.
- (4) Kernel regression over learned embeddings of members of discrete dimensions for incorporating information from related time-series. This easily extends to multiple dimensions.

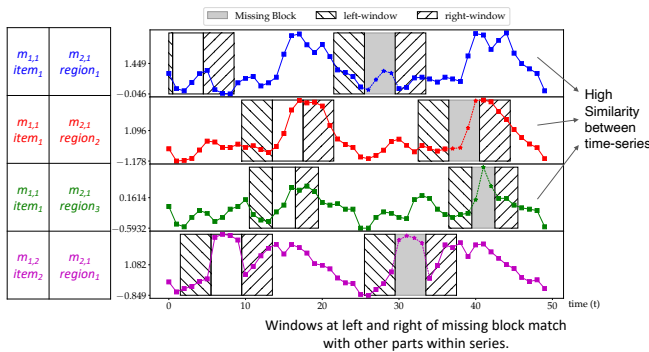


Figure 1: Grey-shaded regions denote missing blocks. Patterns of left and right windows around each missing block match with another part of the same series. Series 1-3 have high similarity and series 1,2,4 show good window match along time.

1.1 Contributions

(1) We propose DeepMVI a carefully designed neural architecture for scalable and accurate imputation of missing values in multidimensional time-series. (2) Our network includes a number of novel design elements to exploit signals from fine-grained and coarse grained temporal patterns within a series and across related series. Our method of extracting relatedness extends naturally to multidimensional datasets, that none of the existing methods handle. (3) We achieve 20–70% reduction in imputation error as shown via an extensive comparison with both state of the art neural approaches and traditional approaches across nine real-life datasets and five different patterns of missing values. (4) Our method is six times faster than using off-the-shelf deep-learning components for MVI. (5) We present the impact of our missing value imputation on downstream aggregate statistics commonly used in data analytics. We show that

existing methods could perform worse than not imputing missing values, whereas ours is the first method that is always better.

2 PRELIMINARIES AND RELATED WORK

We present a formal problem statement, discuss related work, and provide background on relevant neural sequence models.

2.1 Problem Statement

We denote our multidimensional time series dataset as an $n + 1$ dimensional data tensor of real values $X \in \mathbb{R}^{n+1}$. The dimensions of X are denoted as $(K_1, K_2, \dots, K_n, T)$. The dimension T denotes a regularly spaced time index which, without loss of generality we denote as $\{1, \dots, T\}$. Each K_i denotes a categorical dimension comprising of a discrete set of members $\{m_{i,1}, \dots, m_{i,|K_i|}\}$. For example, a retail sales data might consist of two such dimensions: K_1 comprising of items sold and K_2 comprising of regions where they are sold. We denote a specific combination of members of each categorical dimension as $\mathbf{k} = k_1, \dots, k_n$ where each $k_i \in K_i$. We refer to the value at a combination \mathbf{k} and time t as $X_{\mathbf{k},t}$. For example in Figure 1 we show four series of length 50 and their index \mathbf{k} sampled from a two dimensional categorical space of items and regions. We are given an X with some fraction of values $X_{\mathbf{k},t}$ missing. Let M and A be tensors of only ones and zeros with same shape as X that denote the missing and available values respectively in X . We use $\mathcal{I}(M)$ to denote all missing values' (\mathbf{k}, t) indices. The patterns in $\mathcal{I}(M)$ of missing index combinations can be quite varied — for example missing values may be in contiguous blocks or isolated points; across time-series the missing time-ranges may be overlapping or missing at random; or in an extreme case called Blackout a time range may be missing in all series. Our goal is to design a procedure that can impute the missing values at the given indices M so that the error between the imputed values \hat{X}_M and original values X_M is minimized.

$$\sum_{(\mathbf{k}, t) \in \mathcal{I}(M)} \mathcal{E}(\hat{X}_{\mathbf{k},t}, X_{\mathbf{k},t}) \quad (1)$$

where \mathcal{E} denotes error functions such as root mean square error (RMSE) and mean absolute error (MAE). As motivated in Figure 1 both patterns within and across a time series may be required to fill a missing block.

2.2 Related Work

Missing value imputation in time series is an age-old problem [15], with several solutions that we categorize into matrix-completion methods, conventional statistical time-series models, and recent deep learning methods (discussed in Section 2.4). However, all these prior methods are for single-dimensional series. So, we will assume $n = 1$ for the discussions below.

Matrix completion methods These methods [1, 10, 18, 19, 23, 27], view the time-series dataset as a matrix X with rows corresponding to series and columns corresponding to time. They then apply various dimensional reduction techniques to decompose the matrix as $X \approx UV^T$ where U and V represent low-dimensional embeddings of series and time respectively. The missing entry in a series i and position t is obtained by multiplying the corresponding

embeddings. A common tool is the classical Singular Value Decomposition (SVD) and this forms the basis of three earlier techniques: SVDimp[23], SoftImpute [18], and SVT [1]. All these methods are surpassed by a recently proposed centroid decomposition (CD) algorithm called CDRec[10]. CDRec performs recovery by first using interpolation/extrapolation to initialize the missing values. Second, it computes the CD and keeps only the first k columns of U and V , producing U_k and V_k , respectively. Lastly, it imputes values using $X = U_k V_k^T$. This process iterates until the normalized Frobenius norm between the matrices before and after the update reaches a small threshold.

A limitation of pure matrix decomposition based methods is that they do not capture any dependencies along time. TRMF[27] proposes to address this limitation by introducing a regularization on the temporal embeddings V so that these conform to auto-regressive structures commonly observed in time-series data. STMVL is another algorithm that smooths along time and is designed to recover missing values in spatio-temporal data using collaborative filtering methods for matrix completion.

Statistical time-series models DynaMMO[13], is an algorithm that creates groups of a few time series based on similarities that capture co-evolving patterns. They fit a Kalman Filter model on the group using the Expectation Maximization (EM) algorithm. The Kalman Filter uses the data that contains missing blocks together with a reference time series to estimate the current state of the missing blocks. The recovery is performed as a multi-step process. At each step, the EM method predicts the value of the current state and then two estimators refine the predicted values of the given state, maximizing a likelihood function.

We present an empirical comparison with SVDimp (as a representative of pure SVD methods), CDRec, TRMF, STMVL, and DynaMMO and show that our method significantly outperforms all of them on accuracy.

2.3 Background on Neural Sequence Models

We review¹ two popular neural architectures for processing sequence data.

2.3.1 Bidirectional Recurrent Neural Networks. Bidirectional RNN [8] is a special type of RNN that captures dependencies in a sequence in both forward and backward directions. Unlike forecasting, context in both forward and backward directions is available in MVI task. Bidirectional RNN maintains two sets of parameters, one for forward and another for backward direction. Given a sequence X , the forward RNN maintains a state \mathbf{h}_t^f summarizing $X_1 \dots X_{t-1}$, and backward RNN maintains a state \mathbf{h}_t^b summarizing $X_T \dots X_{t+1}$. These two states jointly can be used to predict a missing value at t . Because each RNN models the dependency along only one direction, a bidirectional RNN can compute loss at each term in the input during training.

2.3.2 Transformers. A Transformer [24] is a special type of feed-forward neural network that captures sequential dependencies through a combination of self-attention and feed-forward layers. Transformers are primarily used on text data for language modelling

and various other NLP tasks [5], but have recently also been used for time-series forecasting [14].

Given an input sequence X of length T , a transformer processes it as follows: It first embeds the input X_t for each $t \in [1, T]$ into a vector $E_t \in \mathbb{R}^p$, called the input embedding. It also creates a positional encoding vector at position t denoted as $e_t \in \mathbb{R}^p$.

$$e_{t,r} = \begin{cases} \sin(t/10000^{\frac{r}{p}}), & \text{if } r\%2 == 0 \\ \cos(t/10000^{\frac{r-1}{p}}), & \text{if } (r-1)\%2 == 0 \end{cases} \quad (2)$$

Then it uses linear transformation of input embedding and positional encoding vector to create query, key, and value vectors.

$$Q_t = (E_t + e_t)W^Q \quad K_t = (E_t + e_t)W^K \quad V_t = (E_t + e_t)W^V \quad (3)$$

where the W s denote trained parameters. Key and Value vectors at all times $t \in [1, T]$ are stacked to create matrices K and V respectively. Then the query vector at time t and keys pair at other positions $t' \neq t$ are used to compute a self-attention distribution, which is used to compute a vector at each t as an attention weighted sum of its neighbors as follows:

$$\mathbf{h}_t = \text{Softmax}\left(\frac{Q_t K^T}{\sqrt{p}}\right)V \quad (4)$$

Such self-attention can capture the dependencies between various positions of the input sequence. Transformers use multiple such self-attentions to capture different kinds of dependencies, and these are jointly referred as multi-headed attention. In general, multiple such layers of self-attention are stacked. The final vector \mathbf{h}_t at each t presents a contextual representation of each t .

For training the parameters of the transformer, a portion of the input would be masked (replaced by 0). We denote the masked indices by M . The training loss is computed only on the masked indices in M . This is because multiple layers of self-attention can compute \mathbf{h}_t as a function of any of the input values. This is unlike bidirectional RNNs where the forward and backward RNN states clearly demarcate the values used in each state. This allow loss to be computed at each input position. However, transformers are otherwise faster to train in parallel unlike RNNs.

2.4 Related work in Deep-learning

In spite of the recent popularity and success of deep learning (DL) in several difficult tasks, existing work on the MVI task are few in number. Also there is limited evidence of DL methods surpassing conventional methods across the board. MRNN[26] is one of the earliest deep learning methods. MRNNs use Bidirectional RNNs to capture context of a missing block within a series, and capture correlations across series using a fully connected network. However, a detailed empirical evaluation in [11] found MRNN to be orders of magnitude slower than above matrix completion methods, and also (surprisingly) much worse in accuracy. More recently, BRITS[3] is another method that also uses bidirectional RNNs. At each time step t the RNN is input a column $X_{:,t}$ of X . The RNN state is the black box charged with capturing both the dependencies across time and across series. GP-VAE[7] adds more structure to the dependency by first converting each data column $X_{:,t}$ of X to a low-dimensional embedding, and then using a Gaussian Process to capture dependency along time in the embedding space. Training is via an elaborate structured variational method. On record time

¹Readers familiar with Deep Learning may skip this subsection.

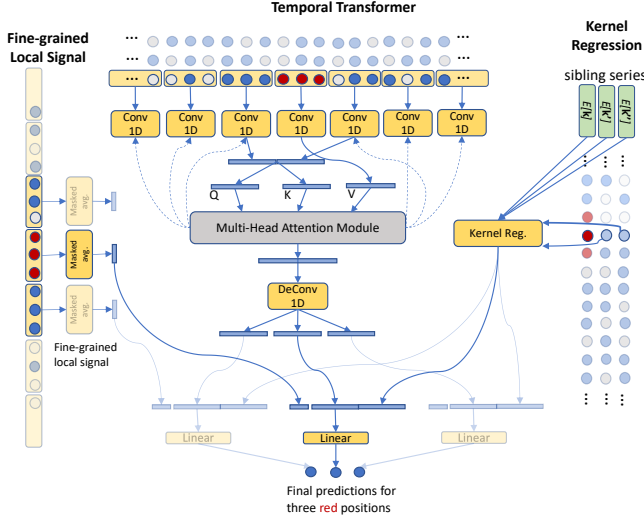


Figure 2: Architecture of DeepMVI. Here model is shown imputing the three circles marked in red at the top. The temporal transformer convolves on window of size $w = 3$ to create queries, keys and values for the multi-headed attention. The deconvolution creates three vectors, one for each red circle. These are concatenated with fine-grained signal and kernel regression to predict the final output.

series datasets GP-VAE has been shown to be worse empirically than BRITS, and seems to be geared towards image datasets.

Compared to these deep models, our network architecture is more modular and light-weight in design, allows for more stable training without dataset specific hyper-parameter tuning, more accurate, and significantly faster.

Other Deep Temporal Models Much of the work on modeling time series data has been in the context of the forecasting task. State of the art methods for forecasting are still RNN-based [4, 6, 21, 22]. The only exceptions is [14] that uses convolution to extract local context features of the time-series and then a transformer to capture longer-range features. Such transformer and convolutions models have been quite successful in speech transcription literature [12]. Our architecture is also based on transformers and convolutions but our design of the keys and queries is better suited for missing value imputation. Further, we also include a fine-grained context and a second kernel regression model to handle across time correlations.

3 THE DEEPMVI MODEL

Our approach to missing value imputation is to train a multi-layered neural network over known values of X and use the trained network to predict the missing values. The network is designed to depend less on parameters, and more on signals derived from a missing block’s context so that its training is light and less prone to over-fitting on small X . Broadly, the three modules of our network are:

- (1) A temporal transformer to extract signals from within a series,

- (2) Multidimensional kernel regression to extract signals from related series, and
- (3) Final output layer to combine results from above two.

A pictorial depiction of our pipeline appears in Figure 2. We describe module’s architecture next and then in Section 3.4 discuss how all parameters are jointly trained.

3.1 Temporal Transformer Across Time

We start with the observation that dependency along time for the missing value imputation task is better captured using a Transformer [24] architecture than a bidirectional Recurrent Neural Networks used in existing deep learning models for MVI [3, 26]. The self-attention in transformers can more easily adapt to missing blocks of data by masking rather than states in RNNs. However, our initial attempts at using the vanilla Transformer model (described in Sec 2.3.2) for the MVI task was subject to over-fitting on long time-series, and inaccurate for block missing values. We designed a new transformer specifically suited for the MVI task which we call the Temporal Transformer. We describe the different stages of this network next.

Our temporal transformer operates on chunks of X at a time, but to avoid notation clutter we continue to refer them as X . We use A to denote all the indices that are not missing in X .

Window-based Feature Extraction Given a series X of length T , in DeepMVI, we first apply 1D Convolution on non-overlapping windows of size w :

$$\mathbf{h}^{\text{conv}} = \text{CONV}_{\theta_{\text{conv}}}(X, w, p) \quad (5)$$

where p denotes number of convolutional filters. The stride in our convolution is equal to window size. This gives us $c = \frac{T}{w}$ windows each represented by a feature of length p . Hence, $\mathbf{h}^{\text{conv}} \in \mathbb{R}^{c \times p}$. For each window $j \in 1 \dots c$ $\mathbf{h}_j^{\text{conv}}$ represents properties of measures at time indices $[t_{(j-1)c+1}, t_{jc}]$. Such a convolution effectively summarizes a local window into a vector of size p . As we will see later, this is useful for the attention module to capture long-range dependencies and not rely on local context alone to predict the missing value. Another advantage is that the length of the sequence has shrunk by w which greatly helps to reduce computation time in the following self-attention phase.

Query, Key, and Value Query and Key vectors in self-attention are crucial in order to capture dependencies that are useful for the task. In vanilla transformer architecture, it suffices to use linear transformations of input embeddings as queries and keys. However, because patterns in time-series emerge at window-level and not at fine-grained level, queries and keys derived from convolution output are more effective.

We create queries and keys in a special way that is more effective for imputation task. Our query and key vector for attention at position j are concatenations of features \mathbf{h}^{conv} at window $j - 1$ to its left and window $j + 1$ to its right. Additionally, following standard Transformer architecture, we encode a position $j \in 1 \dots c$ as a $2p$ -dimensional positional encoding vector e_j using Eq. 2.

$$\mathbf{r}_j = [\mathbf{h}_{j-1}^{\text{conv}}, \mathbf{h}_{j+1}^{\text{conv}}] + e_j \quad (6)$$

See Figure 1 for an illustration of how patterns in the left and right window of a missing block match other time ranges where data is available.

We generate multiple queries and keys for multi-headed attention, using linear transformations over the concatenated vector. For each head $l = 1 \dots n_{\text{head}}$ we get:

$$Q_l = \mathbf{r}W_l^Q \quad K_l = \mathbf{r}W_l^K \quad V = \mathbf{h}^{\text{conv}} \quad (7)$$

where $W_l^Q \in \mathbb{R}^{2p \times 2p}$, $W_l^K \in \mathbb{R}^{2p \times 2p}$.

Compare our method of creating keys with the old method in Eq 3. We use the left-side-window and right-side-window of a block (Figure 1), and not the values at j which may be missing. From j we only include the position features which helps us capture any regular periodicity in the data. This makes our model more suitable for imputation on time-series data. A second difference is that we do not learn embeddings E_t for each input position. When we tried to train time-embeddings, we found that the model was prone to over-fitting. Also, keys derived from poorly trained embeddings were not able to correctly attend to relevant patterns within a series. Also, time embeddings cannot be trained in scenarios like blackout, where all series have a missing block at the same time range. Another advantage is that the number of parameters in our convolution filters is constant and independent of the length of the time-series.

Attention Weighted Context With our keys and queries, we use the same logic as in standard attention to compute a contextual vector for each position j with n_{head} heads as follows:

$$a_l(\mathbf{h}^{\text{conv}}) = \text{Softmax}\left(\frac{Q_l K_l^T}{\sqrt{2p}}, \text{mask} = A^{\text{rand}}\right) V \quad l = 1 \dots n_{\text{head}} \quad (8)$$

$$\mathbf{h}^{\text{mha}} = \text{Concat}[a_1(\mathbf{h}^{\text{conv}}), \dots, a_{n_{\text{head}}}(\mathbf{h}^{\text{conv}})] \quad (9)$$

We use a mask A^{rand} to control the subset of positions over which we attend. In test mode $A^{\text{rand}} = A$, the available positions in X . During training we set A^{rand} to additionally drop random windows around t so as to be robust to missing data. Let b be the average size of the missing block in the data. We sample $v \in [1, \frac{b}{w}]$ and disable the attention in the range $[j - v, j + (\frac{b}{w} - v)]$ for each window j . This way the attention module relies more on values outside the $\frac{b}{w}$ -sized block around each t .

Feed-Forward Network We pass the output of the attention through a feed-forward layer network of single hidden layer of size $d_{\text{feed}} = 512$ and output layer of size $d_{\text{out}} = 32$.

$$\mathbf{h}^{\text{ff}} = \text{ReLU}(W_2(\text{ReLU}(W_1(\text{ReLU}(\mathbf{h}^{\text{mha}})))))) \quad (10)$$

where $W_1 \in \mathbb{R}^{p n_{\text{head}} \times d_{\text{feed}}}$, $W_2 \in \mathbb{R}^{d_{\text{feed}} \times d_{\text{out}}}$, and $\mathbf{h}^{\text{ff}} \in \mathbb{R}^{c \times d_{\text{out}}}$.

Deconvolution Finally the transposed convolution is applied on sequence of states \mathbf{h}^{ff} to obtain the output of the convolution+attention module.

$$\mathbf{h} = \text{CONVT}_{\theta_{\text{convt}}}(\mathbf{h}^{\text{ff}}, w, d_{\text{out}}, 1) \quad (11)$$

where $\mathbf{h} \in \mathbb{R}^{T \times d_{\text{out}}}$.

Fine-grained Local Signal Module For point missing values, the immediately adjacent values might be highly useful which the above window-level attention ignores. We therefore added a second light fine-grained local signal. Each $t \in [1, T]$ is part of window $j = \lfloor \frac{t}{w} \rfloor$. Let start and end times of this window be t_s^j and t_e^j respectively. Then, our fine-grained signal is average of all measure values in $X_{t_s^j}$ to $X_{t_e^j}$, except a randomly selected block of size b .

$$\mathbf{h}_t^{\text{fg}} = \frac{1}{w-b} \left[\sum_{r=t_s^j}^{t_s^j+(t-v)} X_r + \sum_{r=t+(b-v)}^{t_e^j} X_r \right] \quad (12)$$

where $v \sim \text{Uniform}[1, b]$

We create a matrix of all fine-grained signal values as $\mathbf{h}^{\text{fg}} \in \mathbb{R}^{T \times 1}$.

The concatenation of \mathbf{h} from the coarse-grained attention and \mathbf{h}^{fg} from the fine-grained signal forms the final output \mathbf{h}^{tr} of the temporal transformer layer. For each t , the vector \mathbf{h}_t^{tr} is derived from X values at positions other than t . Further during training it also stochastically avoids a block of b values around t . These two properties allow us to train the network by imposing a loss at each available $t \in A$. In contrast, in vanilla transformer since the final vector includes the influence of input embedding at t , loss can be imposed only at pre-decided masked positions of the input.

3.2 Kernel Regression Across Series

We next seek to exploit signal from related series along each of the n categorical dimensions. A series in our case is associated with an n dimensional index $\mathbf{k} = k_1, \dots, k_n$. Recall each dimension is associated with a set of categorical members. We represent relatedness of two members on a dimension as a kernel measuring the similarity of their learned embeddings. Using this kernel, we predict n values at each position \mathbf{k}, t using kernel regression along each of the n categorical dimensions. We present the detailed steps below:

Index Embeddings First, for each categorical member m_{ij} of each dimension K_i , we associate a d_i dimensional learned embedding vector $E[m_{ij}]$.

We define relatedness among series pairs. We only consider series pairs that differ in exactly one dimension. We call these sibling series:

Defining Siblings Siblings for an index \mathbf{k} along categorical dimension i , $S(\mathbf{k}, i)$ is defined as the set of all indices \mathbf{k}' such that \mathbf{k} and \mathbf{k}' differ only at i -th dimension.

$$S(\mathbf{k}, i) = \{\mathbf{k}' : k'_j = k_j \forall j \neq i \wedge k'_i \neq k_i\} \quad (13)$$

For example, in a retail sales data, that contains three items $\{i_0, i_1, i_2\}$ and four regions $\{r_0, r_1, r_2, r_3\}$, siblings of an (item, region) pair $\mathbf{k} = (i_1, r_2)$ along the product dimension would be $S(\mathbf{k}, 0) = \{(i_0, r_2), (i_2, r_2)\}$ and along the region dimension would be $S(\mathbf{k}, 1) = \{(i_1, r_0), (i_1, r_1), (i_1, r_3)\}$.

Regression along each dimension An RBF Kernel computes the similarity score $\mathcal{K}(k_i, k'_i)$ between indices k_i and k'_i in the i -th dimension:

$$\mathcal{K}(k_i, k'_i) = \exp\left(-\gamma * \|E[k_i] - E[k'_i]\|_2^2\right) \quad (14)$$

```

1: procedure DEEPMVI( $X, A, M$ )
2:    $X \leftarrow \frac{X - X_\mu}{X_\sigma}$  //  $X_\mu$ =mean and  $X_\sigma$ =std.dev along time.
3:    $P_{BS}, P_{BO} \leftarrow$  statistics of missing block sizes in  $X$ .
4:    $A^{\text{trn}}, M^{\text{val}} \leftarrow$  MakeValidation( $X, P_{BS}$ ) (Sec. 3.4.1)
5:   model  $\leftarrow$  CreateModel() /* Sec. 3.4.6 */
6:   for iter = 0 to MaxIter do
7:     /* Sec. 3.4.2 and 3.4.3 */
8:     for each ( $\mathbf{k}, t, bs$ )  $\sim$  Batch( $\mathcal{I}(A^{\text{trn}}), P_{BS}$ ) do
9:        $\mathcal{I}^{\text{impute}} \leftarrow \{(\mathbf{k}, t - cs) \dots (\mathbf{k}, t + cs)\}$ 
10:       $\hat{X}_{\mathcal{I}^{\text{impute}}} \leftarrow$  ForwardPass( $\mathcal{I}^{\text{impute}}$ )
11:      Compute Loss  $\forall (\mathbf{k}, t) \in \mathcal{I}^{\text{impute}}$  (Eq. 20).
12:      Update model parameters  $\Theta$ .
13:      Evaluate Stopping Criteria on  $\mathcal{I}(M^{\text{val}})$  (Sec. 3.4.4).
14:      /* Impute test-blocks */
15:       $\hat{X} \leftarrow$  ForwardPass( $\mathcal{I}(M)$ ) over all test blocks in  $\mathcal{I}(M)$ .
16:       $\hat{X} \leftarrow (\hat{X})X_\sigma + X_\mu$ 
17: return  $\hat{X}$ 
18: procedure FORWARDPASS( $\mathcal{I}^{\text{impute}}$ )
19:    $X_{sib} \leftarrow$  Siblings of  $\mathbf{k}$  along each  $i = 1 \dots n$  dimensions.
20:    $\hat{X} \leftarrow$  Adaptive Forward Pass( $\mathcal{I}^{\text{impute}}$ ) (Refer Sec. 3.4.5)
21: return  $\hat{X}$ 
    
```

Figure 3: The DeepMVI training and imputation algorithm

Given a series X at index (\mathbf{k}, t) , for each dimension i , we compute the kernel-weighted sum of measure values as

$$U(\mathbf{k}, i, t) = \frac{\sum_{\mathbf{k}' \in S(\mathbf{k}, i)} \bar{X}_{\mathbf{k}', t} \mathcal{K}(k_i, k'_i) A_{\mathbf{k}', t}}}{\sum_{\mathbf{k}' \in S(\mathbf{k}, i)} \mathcal{K}(k_i, k'_i) A_{\mathbf{k}', t}} \quad (15)$$

where $A_{\mathbf{k}', t} = 1$ for non-missing indices and 0 for missing indices.

When a categorical dimension i is large, we make the above computation efficient by pre-selecting the top L members based on embedding similarity. Let the matrix $U \in \mathbb{R}^{c \times n}$ denote the kernel-weighted sum of measure values for each time index and each sibling dimension for a given \mathbf{k} .

We also compute two other measures: the sum of kernel weights $W \in \mathbb{R}^{c \times n}$ and the variance in the X values along each sibling dimension $V \in \mathbb{R}^{c \times n}$ as follows:

$$W(\mathbf{k}, i, t) = \sum_{\mathbf{k}' \in S(\mathbf{k}, i)} \mathcal{K}(k_i, k'_i) A_{\mathbf{k}', t} \quad (16)$$

$$V(\mathbf{k}, i, t) = \text{Var}(\bar{X}_{S(\mathbf{k}, i), t}) \quad (17)$$

The last layer of the kernel-regression module is just a concatenation of matrices U, V , and W :

$$\mathbf{h}^{\text{kr}} = \text{Concat}(U, V, W) \quad (18)$$

where $\mathbf{h}^{\text{kr}} \in \mathbb{R}^{c \times 3n}$.

3.3 Final Output Layer

The output layer combines states of both attention module and kernel-regression module to obtain the final prediction. We compute the final prediction at position t in X as

$$\hat{X}_t = \mathbf{w}_o^T [\mathbf{h}_t^{\text{tr}}, \mathbf{h}_t^{\text{kr}}] + \mathbf{b}_o \quad (19)$$

3.4 Parameter training and Imputation

The parameters of the network span the temporal transformer, the embeddings of categorical dimensions used in the kernel regression, and the parameters of the output layer. We use Θ to denote all the trainable parameters in all modules:

$$\Theta = \{\theta_{\text{conv}}, \theta_{\text{convt}}, W^Q, W^K, W_1, W_2, \mathbf{w}_o, \mathbf{b}_o, E[m, \cdot]\}.$$

These are trained jointly so that the predicted imputations of available positions A are close to their actual values X . The trained parameters are then used to impute the values in missing positions. The overall pseudocode appears in Figure 3.

During training we start with an X with missing value positions denoted by M to be filled by our method. First, we extract the distribution P_{BS} of missing blocks in M along time and P_{BO} the fraction of total series length that are Blackouts in M .

3.4.1 Set aside validation split. In order to regularize the parameter training process, we then set-aside roughly 10% of X as a validation dataset. The size of the missing blocks in the validation set is set to be the same as the average missing block size in M , but upper bounded by w . The time indices in the validation constitute the mask M^{val} .

3.4.2 Training Loop. Let $\mathcal{I}(A^{\text{trn}}) = \mathcal{I}(A) - \mathcal{I}(M^{\text{val}})$ denote all indices that are available for training parameters. The training loop uses batch stochastic gradient for optimizing the parameters. In each loop, a random subset of X , called a batch B is sampled. The exact method that we used for sampling a batch is detailed in the next paragraph. The training objective is to minimize the MAE between $\hat{X}_{\mathbf{k}, t}$ and $X_{\mathbf{k}, t}$.

$$\Theta^* = \underset{\Theta}{\text{minimize}} \mathbb{E}_{(\mathbf{k}, t) \in \text{Batch}(\mathcal{I}(A^{\text{trn}}))} [\mathcal{E}(\hat{X}_{\mathbf{k}, t}, X_{\mathbf{k}, t})] \quad (20)$$

where Θ denotes model parameters and $\text{Batch}(\mathcal{I}(A^{\text{trn}}))$ denotes our method of selecting a batch from the available training indices that we elaborate next. Before feeding to the model, each series is standard normalised i.e. each (\mathbf{k}, \cdot) has zero mean and unit standard deviation post normalization. The loss is on un-normalised time series i.e. we multiply the standard deviation and add the mean before computing the loss. An off-the-shelf optimization (Adam in our case with a learning rate 1e-2) updates the model parameters using gradients of the above loss.

3.4.3 Method of creating a training batch. A batch is created by first sampling batch-size B indices (\mathbf{k}, t) from available indices $\mathcal{I}(A^{\text{trn}})$. Since our goal is to train for imputing known missing blocks M , we stochastically try to simulate a similar missing pattern around each \mathbf{k}, t both along time and across series. For each batch we sample two values for this: (1) a block size $bs \sim P_{BS}$ and pretend to impute value at (\mathbf{k}, t) assuming a block of size bs along time is missing around it. (2) a binomial value bo with probability P_{BO} . When bo is one we pretend that the same bs -sized block is missing in the siblings of \mathbf{k} . Since X may contain very long time series in general, in order to avoid the quadratic penalty of self-attention, we choose a fixed chunk size cs of length that we include around t to get the series $(\mathbf{k}, t - cs : t + cs)$. We calculate the chunk size as $cs = 50w$ Hence the input to the time series at any point is at most $2cs$. We also feed the sibling values for the selected time series along each

dimension $\{(S(k, j), t - cs : t + cs), j = 1 \dots n\}$ (see Eq 13) for use in kernel regression.

3.4.4 Stopping Criteria. In the training loop, after every 100 batch of parameter updates, we evaluate the imputation loss on the validation dataset. The training loop stops when the loss does not drop in three consecutive iterations. The parameter value corresponding to the smallest loss is saved as the final parameters Θ^* .

3.4.5 Adaptive Forward Pass. In the forward pass we compute the imputed value for an index k, t with a block bs around it missing along time and a bo denoting if sibling series have the same time range missing. This involves computing the temporal attention with context features, the fine-grained local signal, and the kernel regression. However, depending on bs, bo some subset of these modules may provide little or no signal. To ensure that these weak signals do not introduce noise, we adaptively disable some subset of our pipelines as follows: If the missing block size bs is too large ($> w$), local values are not available. Hence we disable fine-grained signal and also the Left and Right window features. In rare cases, when bs is larger than even the chunk size, then the whole temporal attention module is disabled. If sibling series have the same time range missing $bo = 1$ we disable kernel regression.

3.4.6 Network size and default hyper-parameters. The window size $w = 10$ by default. For very large missing block sizes (> 100) we use $w = 20$. The batch size is taken to be 64. The number of filters is taken to be 32. The number of attention heads is four and embedding size is taken to be 10 in all our experiments. In deep learning hyper-parameters are hard to avoid but we found that these settings worked well for all datasets and missing value scenarios (more than 50 settings) that we experimented in this paper. We restrained from extensive dataset specific hyper-parameter tuning.

4 EXPERIMENTS

We present results of our experiments on nine datasets under four different missing value scenarios. We compare imputation accuracy of several methods spanning both traditional and deep learning and approaches in Sections 4.3 and 4.4. We then perform an ablation study to evaluate the various design choice of DeepMVI in Section 4.5. In Section 4.6 we compare different methods on running time. Finally, in Section 4.7 highlight the importance of accurate imputation algorithms, showing that downstream analytics on an incomplete matrix would be better than erroneous imputation as those given by baselines.

4.1 Experiment Setup

4.1.1 Datasets. We experiments on eight datasets used in earlier papers on missing value imputation [11]. In addition, due to the lack of multi-dimensional datasets in previous works, we introduce "JanataHack", a new dataset as a representative. Table 1 presents a summary along with qualitative judgements of their properties.

AirQ brings air quality measurements collected from 36 monitoring stations in China from 2014 to 2015. AirQ time series contain both repeating patterns and jumps, and also strong correlations across time series. We use two variants of the dataset in our analysis. Replicating [11] setup, we filter the dataset to get 10 time series of 1000 length and replicating the [3] setup we use the raw dataset

Dataset	Number of TS	Length of TS	Repetitions within TS	Relatedness across series
AirQ	10	1k	Moderate	High
Chlorine	50	1k	High	High
Gas	100	1k	High	Moderate
Climate	10	5k	High	Low
Electricity	20	5k	High	Low
Temperature	50	5k	High	High
Meteo	10	10k	Low	Moderate
BAFU	10	50k	Low	Moderate
JanataHack	76*28	134	Low	High

Table 1: Datasets: All except the last one has one categorical dimension. Qualitative judgements on the repetitions of patterns along time and across series appear in the last two columns.

with train-test split as defined in the paper.

Chlorine simulates a drinking water distribution system on the concentration of chlorine in 166 junctions over 15 days in 5 minutes interval. This dataset contains clusters of similar time series which exhibit repeating trends.

Gas shows gas concentration between 2007 and 2011 from a gas delivery platform of ChemoSignals Laboratory at UC San Diego.

Climate is monthly climate data from 18 stations over 125 locations in North America between 1990 and 2002. These time series are irregular and contain sporadic spikes.

Electricity is on household energy consumption collected every minute between 2006 and 2010 in France.

Temperature contains temperature from climate stations in China from 1960 to 2012. These series are very highly correlated with each other.

MeteoSwiss is weather from different Swiss cities from 1980 to 2018. Meteo time series contain repeating trends with sporadic anomalies.

BAFU consists of water discharge data provided by the BundesAmt Fir Umwelt (BAFU), the Swiss Federal Office for the Environment, collected from different Swiss rivers from 1974 to 2015. These time series contain synchronized irregular trends.

JanataHack is a real life multidimensional time series dataset² which consist of sales data spanning over 130 weeks, for 76 stores and 28 products (termed "SKU"). The dataset is inherently multi-dimensional with (store,product) combination uniquely indexing a time series.

4.1.2 Missing Scenarios Description. We here introduce 4 missing scenarios[11] which are considered to be the common missing patterns encountered in real datasets. The measures here are considered to be missing in continuous chunks of time termed blocks. We also consider scenario where values are missing sparsely throughout the dataset in Section 4.4.

Missing Completely at Random (MCAR) Each incomplete time series has 10% of its data missing. The missing data is in

²<https://www.kaggle.com/vin1234/janatahack-demand-forecasting-analytics-vidhya>

randomly chosen blocks of constant size 10. We experiment with different % of incomplete time series to present our numbers.

Missing Disjoint (MissDisj) Here we consider disjoint blocks to be missing from the incomplete series. Block size is T/N , where T is the length of time series, and N is the number of time series. For i th time series the missing block ranges from time step $\frac{iT}{N}$ to $\frac{(i+1)T}{N} - 1$, which ensures that given any % of time series incomplete, missing blocks do not overlap across series.

Missing Overlap (MissOver) A slight modification on MissDisj, MissOver has block size of $2 * T/N$ for all time series except the last one for which the block size is still T/N . For i th time series the missing block ranges from time step $\frac{iT}{N}$ to $\frac{(i+2)T}{N} - 1$, which causes an overlap between missing blocks of series i with $i - 1$ and $i + 1$

Blackout considers scenario where all the time series have missing values for the same time range. Given a block size s all time series have values missing from t to $t + s$, where t is fixed to be 5% from the start. We vary s from 10 to 100 to present our results.

4.1.3 Methods Compared. We compare with methods from both conventional and deep learning literature for our baselines.

CDRec[10] is one of the top performing recent Matrix Factorisation based technique which uses iterative Centroid Decomposition.

DynaMMO[13] is a probabilistic method that uses Kalman Filters to model co-evolution of subsets of similar time series.

TRMF [27] is a matrix factorisation augmented with an autoregressive temporal model.

SVDImp [23] is a basic matrix factorisation based technique which reconstructs imputes using top k vectors in V in SVD factorisation. **STMVL** [25] STMVL uses collaborative filtering methods for matrix completion.

MRNN [26] is an early deep learning method that uses a Bidirectional RNN to do imputation in a single time series, and a separate fully connection NN to capture correlations across series.

BRITS [3] is a more recent Deep learning techniques that also uses Bidirectional RNNs but a single RNN is fed all time series as a vector unlike MRNNs.

4.1.4 Other Experiment Details.

Platforms Our experiments are done on the Imputation Benchmark³ for comparisons with conventional methods. The benchmark lacks in support for deep learning based algorithms hence we compare our numbers for those outside this framework.

Evaluation metric We use Mean Absolute Error as our evaluation metric for the goodness of the algorithm.

4.2 Visual Comparison of Imputation Quality

We start with a visual illustration of how DeepMVI’s imputations compare with those of two of the best performing existing methods: CDRec and DynaMMO. In Fig. 4, we visualize the imputations for different missing blocks on the Electricity dataset. First row is for MCAR scenario whereas second row is for Blackout scenario. First observe how DeepMVI(Blue) correctly captures both the shape and scale of actual values (Black) over a range of missing blocks. On

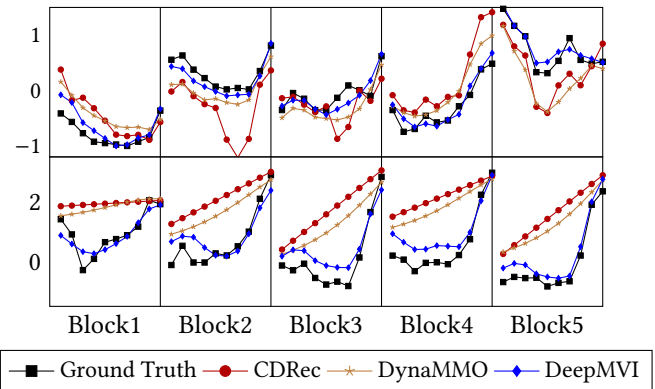


Figure 4: Visualised Imputations on Electricity Dataset. The top row shows MCAR missing blocks while the bottom row is for Blackout scenario.

the MCAR scenario CDRec gets the shape right, only in the first and fourth blocks, however it is off with scale. In the third block, CDRec predicts the sharp decline in the middle. However, this decline occurs in ground-truth of fifth block. DynaMMO correctly captures the shape except for fifth block. However, its scales are slightly worse than DeepMVI in the first four blocks. In the Blackout scenario, CDRec only linearly interpolates the values in missing block, whereas DynaMMO is only slightly inclined towards ground-truth. However, both CDRec and DynaMMO miss the trend during Blackout whereas DeepMVI successfully captures it because of careful pattern match within a series.

4.3 Comparison on Imputation Accuracy

Given the large number of datasets, methods, missing scenarios and missing sizes we present our numbers in stages. First in Figure 5 we show comparisons in MAE of all conventional methods on five datasets under a fixed $x = 10\%$ of series with missing values in MCAR, MissDisj, MissOver and all series in Blackout with a block size of 10. Then, in Figure 6 we show more detailed MAE numbers on three datasets (AirQ, Climate and Electricity) where we vary the percent of series with missing values (x) from 10 to 100 for MCAR, MissDisj, MissOver and the block size from 10 to 100 in Blackout. From these comparisons across eight datasets we make the following observations:

First, observe that DeepMVI is better or comparable to all other methods under all missing values scenarios and all datasets. Our gains are particularly high in the Blackout scenario seen in the last column in graphs in Figure 6 and in the bottom-right graph of Figure 5. For accurate imputation in Blackouts, we need to exploit signals from other locations of the same series. Matrix factorisation based methods such as SVDImp and TRMF fail in doing so and rely heavily on correlation across time series. TRMF’s temporal regularisation does not seem to be helping in capturing long term temporal correlations. DynaMMO and CDRec are able to capture within time series dependencies better than matrix factorisation methods. But they are still much worse than DeepMVI, particularly on Gas in Figure 5, and Climate, Electricity in Figure 6.

³<https://github.com/eXascaleInfolab/bench-vldb20>

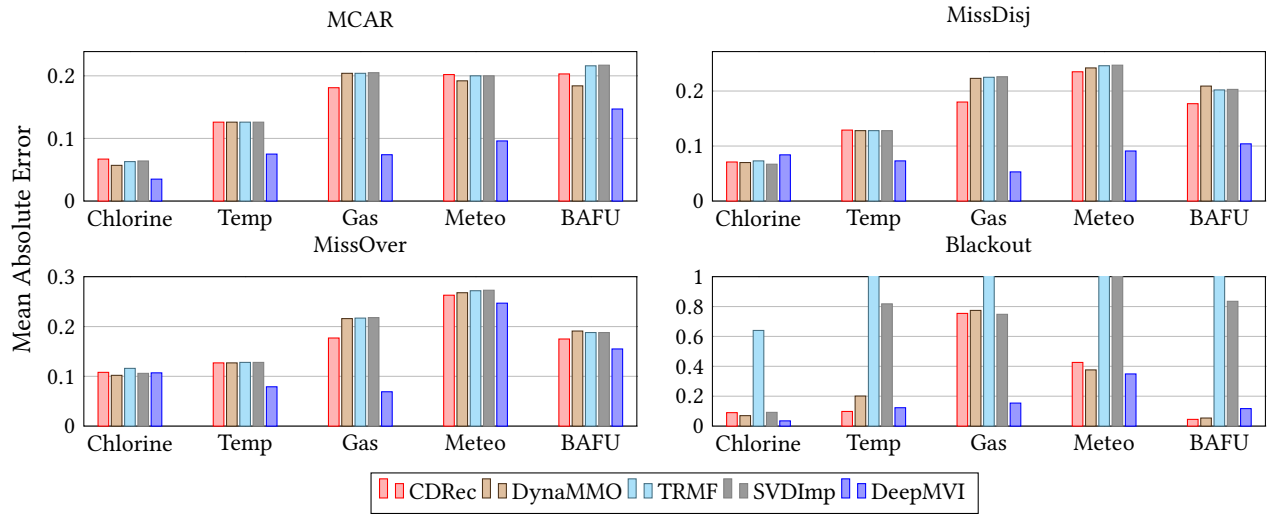


Figure 5: Mean Absolute Errors (y-axis) on five other datasets (on x-axis) on all four scenarios – MCAR, MissDisj, MissOver, and Blackout. Here, a fixed $x = 10\%$ of the series in each dataset has missing blocks.

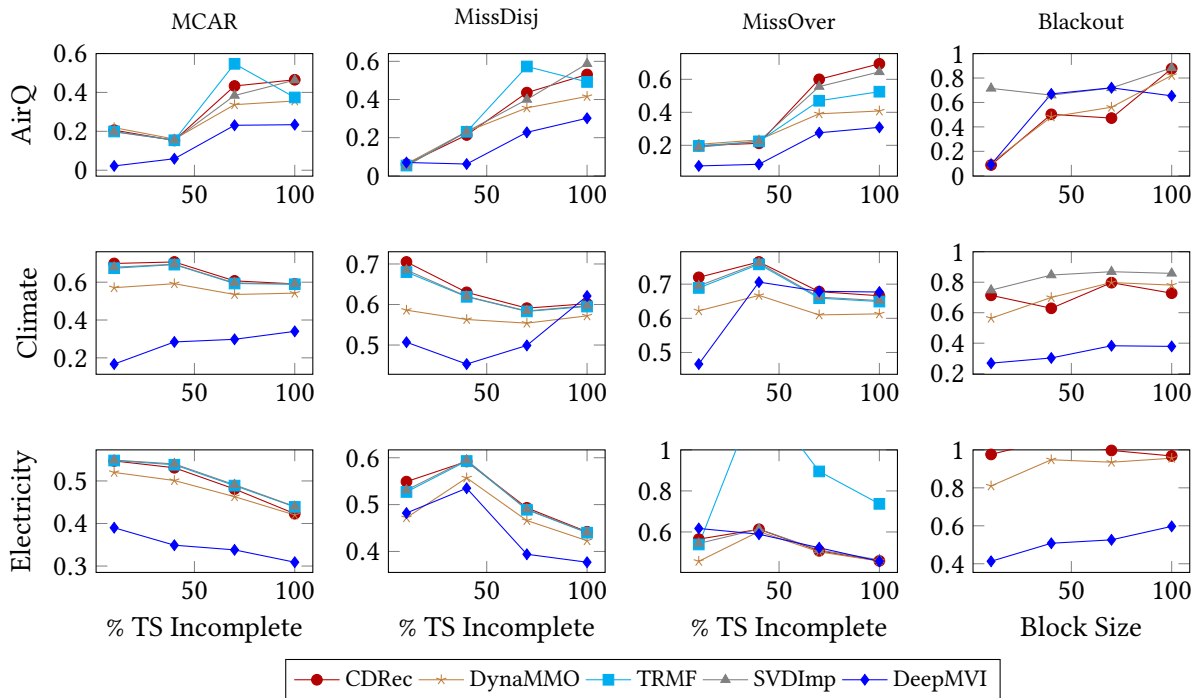


Figure 6: Mean Absolute Errors (y-axis) on three datasets along rows and under four missing scenarios along columns. X-axis is percent of time-series with a missing block for MCAR, MissDisj, MissOver and size of the missing block for Blackout.

In the MissDisj/MissOver scenario where the same time range is not missing across all time series, methods that effectively exploit relatedness across series perform better on datasets with highly correlated series such as Chlorine and Temp. The difference among

the various methods is much smaller here, but even in these scenarios we provide as much as 50% error reduction compared to existing methods.

MCAR is the most interesting scenario for our analysis. Most of the baselines are geared towards capturing either inter or intra TS correlation but none of them are able to effectively combine and

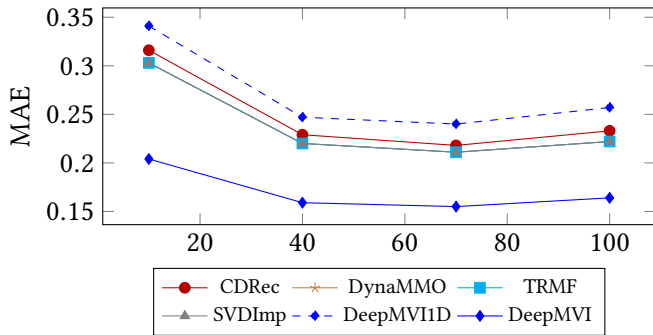


Figure 7: MAE (y-axis) for MCAR scenario on JanataHack. X-axis is percent of time series with missing blocks.

exploit both. MCAR owing to small block size and random missing position can benefit from both inter and intra correlation which are fully exploited by our model. DeepMVI achieves strictly better numbers than all the baselines on all the datasets. Specifically for Climate and Electricity datasets where other methods have high errors, we reduce these errors between 20% and 70% as seen in the first column of Figure 6.

4.3.1 Comparison on the Multidimensional Dataset. We next present comparisons on the JanataHack dataset that consists of two categorical dimensions: product and store. Also, compared to the other eight datasets in Table 1 the length of each series is small (134) and the total number of series is large (2128). For this task, we run two variants of our model. The first model dubbed as DeepMVI1D flattens the multidimensional index of time series by getting rid of the store and product information. The second variant is the proposed model itself which retains the multi-dimensional structure and applies kernel embeddings in two separate spaces. In DeepMVI each time series is associated with two embeddings of size k each. To keep the comparison fair, DeepMVI1D uses embedding of size $2k$. Since other methods have no explicit model for multi-dimensional indices, the input is a flattened matrix, similar to DeepMVI1D.

Figure 7 shows the performance of the variants compared to the baselines on MCAR for increasing percentage x of series with a missing block. Observe how in this case too DeepMVI is significantly more accurate than other methods including DeepMVI1D. If each series is small and the number of series is large, there is a greater chance of capturing spurious correlation across series. In such cases, the external multidimensional structure that DeepMVI exploits helps to restrict relatedness only among siblings of each dimension. We expect this difference to get magnified as the number of dimensions increase.

4.4 Comparison with Deep Learning Methods

We compare our method with two existing deep learning methods: BRITS and MRNN. Since the code of these methods was not available, we are restricted to compare only on the one dataset whose experimental settings we could replicate for our method. The numbers reported in Table 2 are taken from the respective papers. We also include the numbers from a non-deep learning method ST-MVL for reference. Note an earlier study in [11] had

Model Name: method	MAE
BRITS: Bi-RNN on concatenated series [3]	11.56
MRNN: Bi-RNN on single series [26]	14.24
ST-MVL: collaborative filtering [25]	12.12
DeepMVI: Tranformer+KR (Ours)	9.93

Table 2: Comparison with Deep Learning Methods on Beijing AirQuality Dataset.

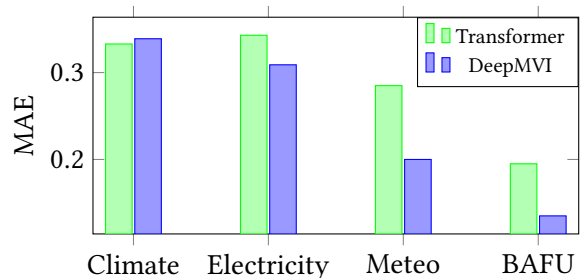


Figure 8: Bar plot showing MAE (y-axis) for different datasets (x-axis) on Transformer and DeepMVI using MCAR scenario with all time series being incomplete. Further details in Section 4.5.1

already concluded that MRNN was significantly worse than non-deep learning methods like CDRec, and in Section 4.3 we showed that DeepMVI is significantly more accurate than CDRec. On this dataset we find that while the more recent BRITS method is more accurate than MRNN, DeepMVI is more accurate than BRITS reducing the MAE from 11.56 to 9.93. Both BRITS and MRNN are based on recurrent neural networks, and the Transformer architecture of DeepMVI is able to better handle missing data. Another difference is that in BRITS the correlation across TS is handled implicitly via the black-box RNN whereas we factorize out this relatedness via member embeddings and kernel regression.

4.5 Justifying Design Choices of DeepMVI

DeepMVI introduces a Temporal transformer with an innovative left-right window feature to capture coarse-grained context, a fine-grained local signal, and a kernel regression module. Here we perform an ablation study to dissect the role of each of these parts.

4.5.1 Role of Windowing. We justify the choice of applying attention on window based feature vectors (Eq. 5) as opposed to scalar values like in vanilla transformers. Fig 8 shows MAE error for this vanilla Transformer model vs DeepMVI on different datasets. We see that a Transformer using attention on measure values (with large enough attention context) can capture periodic correlations within time series such as those in Climate dataset. However it fails to capture more subtle non-periodic repeating pattern which requires attention on window feature vectors instead of measure scalars. Such patterns prevalent in Electricity, Meteo and BAFU see significant reduction in MAE with windowing.

4.5.2 Role of Context Window Features. We next study the role of query/key selected within our Temporal Transformer module.

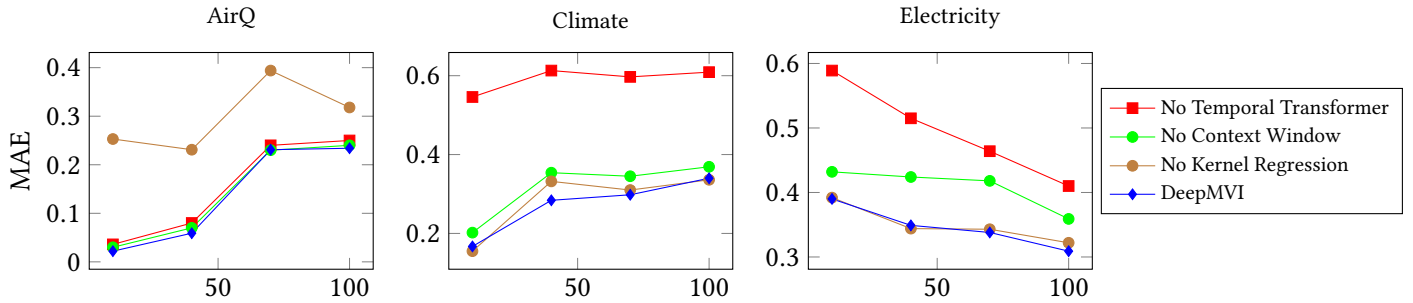


Figure 9: Ablation Study done via 3 datasets represented by different plots AirQ,Climate,Electricity on MCAR scenario. y-axis shows MAE and x-axis % of Missing TS.

Our query/key consists of concatenated window features of previous and next block arithmetically added with positional encoding. Positional encoding encode the relative positions and have no information pertaining to the context of the block where imputation needs to be performed. A question to be asked here was whether the contextual information around a missing block help in a better attention mechanism or whether the attention mechanism just ignores this contextual information doing a fixed periodic imputation. Figure 9 shows this method (Green). These experiments are on MCAR and x-axis is increasing % of missing TS. Comparing the green and blue, we see that our window context features did help on two of the three datasets, with the impact on Electricity being quite significant. This might be attributed to the periodic nature of the climate dataset compared to non-periodic but strongly contextual information in electricity.

4.5.3 Role of Temporal Transformer and Kernel Regression. In Figure 9 we present error without the Temporal Transformer Module(Red) and without Kernel Regression Module(Brown). We see some interesting trends here. On Climate and Electricity where each series is large (5k) with repeated patterns across series, we see that dropping the temporal transformer causes large jumps in error. On Climate error jumps from 0.15 to 0.55 with 10% missing! In AirQ we see little impact. However, on this data dropping Kernel regression causes a large increase in error jumping from 0.04 to 0.25 on 10% missing. kernel regression does not help much beyond temporal transformer on Climate and Electricity. These experiments show that DeepMVI is capable of combining both factors and determining the dominating correlation via the training process.

4.5.4 Role of Fine-Grained Local Signal. (Equation 12). This signal is most useful for small missing blocks. Hence we modify the MCAR missing scenario such that missing percentage from all time series is still 10%, but the missing block size is varied from 1 to 10. Figure 10 shows the results where we compare our MAE with and without fine grained local signal with CDRec algorithm on the Climate Dataset. The plot shows that including fine grained signal helps improve accuracy over a model which ignores the local information. Also the gain in accuracy with fine grained local signal diminishes with increasing block size which is to be expected.

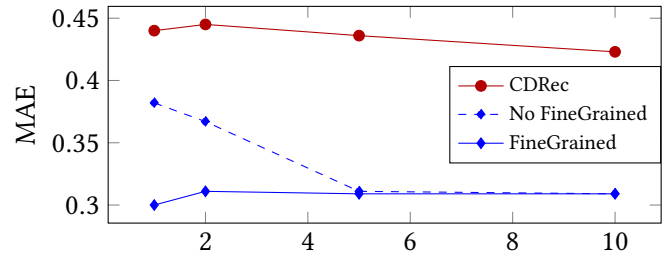


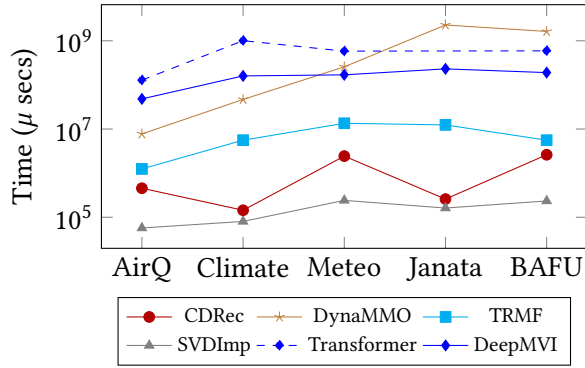
Figure 10: MAE (y-axis) vs missing block size (x-axis) with 10% missing on Climate Dataset. Gains from fine-grained local signal decreases with increasing block size.

4.6 Running Time

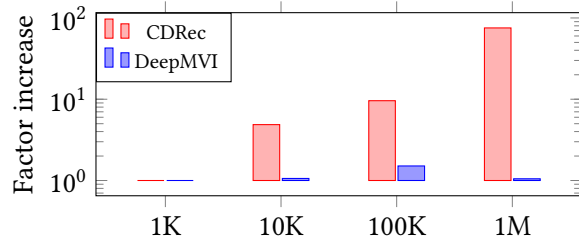
The above experiments have shown that DeepMVI is far superior to existing methods on accuracy of imputation. One concern with any deep learning based solution is its runtime overheads. We show in this section that while DeepMVI is slower than existing matrix factorization methods, it is more scalable with TS length and much faster than off-the-shelf deep learning methods.

We present running times on AirQ, Climate, Meteo, BAFU, and JanataHack datasets in Figure 11a. The x-axis shows the datasets ordered by increasing total size and y-axis is running time in log-scale. In addition to methods above we also show running time with an off the shelf transformer method. Matrix factorisation based method like CDRec and SVDImp are much faster than DynaMMO and DeepMVI. But compared to the vanilla Transformer our running time is a factor of 2.5 to 7 smaller. The running time of DynaMMO exceeds the running time of other algorithms by a factor of 1000 and increases substantially with increasing series length, which undermines the accuracy gains it achieves. On the JanataHack dataset, DynaMMO took 25 mins ($1.5e9 \mu s$) compared to DeepMVI which took just 2.5 mins.

We next present experiments on a Synthetic dataset introduced in [11] to measure scalability. The dataset consists of 10 series of length 1 million each. We take the first t time steps where $t \in 1K, 10K, 100K, 1M$ and plot factor increase in running time normalized wrt running time for sequence length of 1K. We compare here only with CDRec, as when dealing with time series of this scale other methods with decent MAE errors have considerably



(a) Absolute Runtime (μ secs) on y-axis with dataset arranged in increasing data set size. MCAR scenario with all time series having missing blocks ($x=100\%$).



(b) Factor increase (y-axis) in running time on a time series relative to time on series of length 1k. X-axis shows series length. Number of time series is 10. More details in Section 4.6

Figure 11: Runtime Analysis of DeepMVI

larger running as shown in [11]. CDRec is the only scalable model with good accuracy among the non-DL methods [11]. Figure 11b shows that our algorithm scales better than CDRec on increasing time series length and almost seems $O(1)$ wrt series length. The reason is that our training algorithm samples chunks of constant size to learn correlations along time. If the dominant patterns in a time series are invariant of the length of the time series, these can be learned while iterating over a fixed number of chunks.

4.7 Impact on downstream analytics

A major motivation for missing value imputation is more accurate data analytics on time series datasets [2, 9, 17, 20]. Analytical processing typically involves studying trends of aggregate quantities such as averages or average changes. When some detailed data is missing, a default option is to just ignore the missing data from the aggregate statistic. An analyst may ignore an entire series with missing blocks or just the cells which are missing. Any MVI method to be useful should result in more accurate top-level aggregates than just ignoring missing values. We present a comparison of the different MVI methods on two aggregate statistics on X :

- Average over the first categorical dimension so the result is a $n - 1$ dimensional aggregated time series. Except in JanataHack, this results in a single averaged time series.
- Average percent increase in measure from time t to $t + 1$ again on the first dimension.

Datasets-Missing%	True Statistic (Average)	MAE ($\times 100$)				
		CDRec	DynaMMO	DropCell	DropSeries	DeepMVI
		Average percent change from t to $t + 1$				
AirQ-10	-0.0720	0.63	2.01	0.83	0.83	0.14
AirQ-40	0.0022	2.05	0.63	1.56	1.05	0.19
Climate-10	-1.0081	1.72	33.44	11.15	11.15	0.67
Janata-10	0.3025	0.83	1.78	0.70	1.50	1.38
Janata-40	0.3398	2.71	3.11	1.57	9.71	1.56
Average at each t over series						
AirQ-10	-0.0826	0.06	0.11	0.47	0.47	0.06
AirQ-40	-0.1582	0.03	0.03	1.01	6.52	0.07
Climate-10	-0.0351	0.73	0.67	0.71	0.71	0.51
Janata-10	0.6393	0.15	0.16	1.24	4.14	0.12
Janata-40	0.6314	0.32	0.32	0.13	5.79	0.23

Table 3: MAE on two aggregate queries at each t over all series the first categorical dimension. Highlighted cells are worse than either DropCell or DropSeries.

Apart from computing these statistics on the imputation output by various algorithms, we also compute these statistics over the missing data with two variants :

- DropSeries that ignores the entire time series if it has a missing block
- DropCell that ignores time steps with missing values

We consider five missing matrices for this evaluation: AirQ in MCAR with 10% missing, AirQ in MCAR with 40% missing, Climate in MCAR with 10% missing, JanataHack in MCAR with 10% missing, JanataHack in MCAR with 40% missing. Table 3 shows the mean average error (MAE) between the true aggregate and computed aggregate. The cases an imputation method is performing worse than either of the Drop missing methods are highlighted in yellow. We observe that averaged over all ten cases, DeepMVI is the only imputation method that provides overall gains beyond the default of dropping missing entries. This justifies the use of our possibly more compute-heavy imputation method, because existing faster methods could lead to worse analytics than not imputing.

5 CONCLUSION AND FUTURE WORK

In this paper, we propose DeepMVI, a deep learning method for missing value imputation in multi-dimensional time-series data. DeepMVI combines within-series signals using a novel temporal transformer, across-series signals using a multidimensional kernel regression, and local fine-grained signals. The network parameters are carefully selected to be trainable across wide ranges of data sizes, data characteristics, and missing block pattern in the data.

We extensively evaluate DeepMVI on nine datasets, against seven existing methods, and with four missing-value scenarios. DeepMVI achieves up to 70% error reduction compared to state of the art methods. Our method is up to 50% more accurate and six times faster than using off-the-shelf neural sequence models. We also justify our module choices by comparing DeepMVI with its variants. Through two downstream analytics tasks, we show that DeepMVI’s performance on downstream tasks is better than dropping the series with missing values as well as existing methods.

Future work in this area includes applying our neural architecture to other time-series tasks including forecasting.

REFERENCES

- [1] Jian-Feng Cai, Emmanuel J Candès, and Zuowei Shen. 2010. A singular value thresholding algorithm for matrix completion. *SIAM Journal on optimization* 20, 4 (2010), 1956–1982.
- [2] José Cambronero, John K. Feser, Micah J. Smith, and Samuel Madden. 2017. Query Optimization for Dynamic Imputation. *Proc. VLDB Endow.* 10, 11 (2017).
- [3] Wei Cao, Dong Wang, Jian Li, Hao Zhou, Lei Li, and Yitan Li. 2018. Brits: Bidirectional recurrent imputation for time series. *arXiv preprint arXiv:1805.10572* (2018).
- [4] Prathamesh Deshpande and Sunita Sarawagi. 2019. Streaming adaptation of deep forecasting models using adaptive recurrent units. In *Proceedings of the 25th ACM SIGKDD International Conference on Knowledge Discovery & Data Mining*. 1560–1568.
- [5] Jacob Devlin, Ming-Wei Chang, Kenton Lee, and Kristina Toutanova. 2018. BERT: Pre-training of Deep Bidirectional Transformers for Language Understanding. *arXiv preprint arXiv:1810.04805* (2018).
- [6] Valentin Flunkert, David Salinas, and Jan Gasthaus. 2017. DeepAR: Probabilistic Forecasting with Autoregressive Recurrent Networks. *CoRR abs/1704.04110* (2017).
- [7] Vincent Fortuin, Dmitry Baranchuk, Gunnar Rätsch, and Stephan Mandt. 2020. Cp-vae: Deep probabilistic time series imputation. In *International Conference on Artificial Intelligence and Statistics*. PMLR, 1651–1661.
- [8] Alex Graves and Jürgen Schmidhuber. 2005. Framewise phoneme classification with bidirectional LSTM and other neural network architectures. *Neural networks* 18, 5-6 (2005), 602–610.
- [9] Sean Kandel, Ravi Parikh, Andreas Paepcke, Joseph M Hellerstein, and Jeffrey Heer. 2012. Profiler: Integrated statistical analysis and visualization for data quality assessment. In *Proceedings of the International Working Conference on Advanced Visual Interfaces*. 547–554.
- [10] Mourad Khayati, Philippe Cudré-Mauroux, and Michael H Böhlen. 2019. Scalable recovery of missing blocks in time series with high and low cross-correlations. *Knowledge and Information Systems* (2019), 1–24.
- [11] Mourad Khayati, Alberto Lerner, Zakhar Tymchenko, and Philippe Cudré-Mauroux. 2020. Mind the gap: an experimental evaluation of imputation of missing values techniques in time series. *Proceedings of the VLDB Endowment* 13, 5 (2020), 768–782.
- [12] Jason Li, Vitaly Lavrukhin, Boris Ginsburg, Ryan Leary, Oleksii Kuchaiev, Jonathan M Cohen, Huyen Nguyen, and Ravi Teja Gadde. 2019. Jasper: An end-to-end convolutional neural acoustic model. *arXiv preprint arXiv:1904.03288* (2019).
- [13] Lei Li, James McCann, Nancy S Pollard, and Christos Faloutsos. 2009. Dynammo: Mining and summarization of coevolving sequences with missing values. In *Proceedings of the 15th ACM SIGKDD international conference on Knowledge discovery and data mining*. 507–516.
- [14] Shiyang Li, Xiaoyong Jin, Yao Xuan, Xiyu Zhou, Wenhui Chen, Yu-Xiang Wang, and Xifeng Yan. 2019. Enhancing the locality and breaking the memory bottleneck of transformer on time series forecasting. In *Advances in Neural Information Processing Systems*. 5243–5253.
- [15] Roderick JA Little and Donald B Rubin. 2002. Single imputation methods. *Statistical analysis with missing data* (2002), 59–74.
- [16] Yukai Liu, Rose Yu, Stephan Zheng, Eric Zhan, and Yisong Yue. 2019. NAOMI: Non-autoregressive multiresolution sequence imputation. In *Advances in Neural Information Processing Systems*. 11238–11248.
- [17] Chris Mayfield, Jennifer Neville, and Sunil Prabhakar. 2010. ERACER: A Database Approach for Statistical Inference and Data Cleaning. In *Proceedings of the 2010 ACM SIGMOD International Conference on Management of Data*.
- [18] Rahul Mazumder, Trevor Hastie, and Robert Tibshirani. 2010. Spectral regularization algorithms for learning large incomplete matrices. *The Journal of Machine Learning Research* 11 (2010), 2287–2322.
- [19] Jiali Mei, Yohann De Castro, Yannig Goude, and Georges Hébrail. 2017. Nonnegative matrix factorization for time series recovery from a few temporal aggregates. In *International Conference on Machine Learning*. PMLR, 2382–2390.
- [20] Tova Milo and Amit Somech. 2020. Automating exploratory data analysis via machine learning: An overview. In *Proceedings of the 2020 ACM SIGMOD International Conference on Management of Data*. 2617–2622.
- [21] David Salinas, Michael Bohlke-Schneider, Laurent Callot, Roberto Medico, and Jan Gasthaus. 2019. High-dimensional multivariate forecasting with low-rank Gaussian Copula Processes. In *Advances in Neural Information Processing Systems*. 6827–6837.
- [22] Rajat Sen, Hsiang-Fu Yu, and Inderjit Dhillon. 2019. Think globally, act locally: A deep neural network approach to high-dimensional time series forecasting. *arXiv preprint arXiv:1905.03806* (2019).
- [23] Olga Troyanskaya, Michael Cantor, Gavin Sherlock, Pat Brown, Trevor Hastie, Robert Tibshirani, David Botstein, and Russ B Altman. 2001. Missing value estimation methods for DNA microarrays. *Bioinformatics* 17, 6 (2001), 520–525.
- [24] Ashish Vaswani, Noam Shazeer, Niki Parmar, Jakob Uszkoreit, Llion Jones, Aidan N Gomez, Ł ukasz Kaiser, and Illia Polosukhin. 2017. Attention is All you Need. In *NIPS*.
- [25] Xiuwen Yi, Yu Zheng, Junbo Zhang, and Tianrui Li. 2016. ST-MVL: filling missing values in geo-sensory time series data. (2016).
- [26] Jinsung Yoon, William R Zame, and Mihaela van der Schaar. 2018. Estimating missing data in temporal data streams using multi-directional recurrent neural networks. *IEEE Transactions on Biomedical Engineering* 66, 5 (2018), 1477–1490.
- [27] Hsiang-Fu Yu, Nikhil Rao, and Inderjit S Dhillon. 2016. Temporal regularized matrix factorization for high-dimensional time series prediction. In *Advances in neural information processing systems*. 847–855.